Journal of the Ceramic Society of Japan 123 [9] 770-778 2015 Paper

Synthesis of hierarchically porous polymethylsilsesquioxane monoliths with controlled mesopores for HPLC separation

Yang ZHU, Yoshie MORIMOTO, Taiyo SHIMIZU, Kei MORISATO,*
Kazuyuki TAKEDA, Kazuyoshi KANAMORI† and Kazuki NAKANISHI††

Department of Chemistry, Graduate School of Science, Kyoto University, Kitashirakawa, Sakyo-ku, Kyoto 606–8502, Japan
***GL Sciences, Inc., 237–2 Sayamagahara, Iruma, Saitama 358–0032, Japan**

Sol–gel synthesis of macroporous polymethylsilsesquioxane (PMSQ) monoliths has been successful over the past decade, and applications to separation media have been investigated. However, the control of mesopores to tailor hierarchical porosity, which is promising for improvement of the separation efficiency, remains challenging. In particular, an independent control of meso- and macropores has not been achieved in PMSQ. Herein we present a method to synthesize PMSQ monoliths with well-defined macropores and controlled mesostructure (pore size ranging from 10 to 60 nm, total pore volume from 0.2 to 0.6 $cm^3 g^{-1}$) via sol–gel accompanied by phase separation. Different Pluronic-type nonionic surfactants were used to control phase separation of the hydrophobic PMSQ network in aqueous media. Due to different packing density of the colloidal PMSQ constituents in the continuous skeletons in the micrometer-scale (termed as macropore skeletons) and their rearrangements through the hydrothermal post-treatment under basic conditions, mesopore characteristics have been successfully controlled independently of the preformed macropore structure. Separation columns for high-performance liquid chromatography (HPLC) have been fabricated using the PMSQ monoliths, and acceptable separation performances in both the reversed-phase and normal-phase modes have been demonstrated due to the presence of both hydrophilic silanol groups and hydrophobic methyl groups.

Key-words : Sol–gel, Porous materials, Hierarchical porosity, Monoliths, Polymethylsilsesquioxane, Separation media

[Received March 12, 2015; Accepted June 27, 2015]

1. Introduction

Porous polyorganosiloxanes (so-called organosilica or hybrid silica) with various functionalities are an important category of materials for catalysts, catalyst supports, adsorbents and separation media.[1)–3)] Although the most frequently employed method to obtain such functionalized materials, surface functionalization of silica, is proven to be simple and versatile,[2),4)–9)] the direct synthesis from organoalkoxysilanes including organotrialkoxysilanes and organo-bridged alkoxysilanes[10)–13)] with target functional groups provides distinguished materials that offer unique properties such as better alkaline resistivity and improved mechanical properties as compared to silica.

One of the most-studied functional polyorganosiloxane systems is polymethylsilsesquioxane (PMSQ with ideal composition of $CH_3SiO_{1.5}$). Due to the presence of large amount of hydrophobic and less polarizable methyl groups, PMSQ materials are applied in an extended field and recent studies include hydrophobic coatings,[14)] stationary phase for chromatography[15)] and ultralow-*k* dielectric films.[16)] The PMSQ materials have also been regarded as an important precursor to silicon oxycarbide ceramics.[17)] In some cases, such as low-density PMSQ aerogels, elastic properties associated with high compressive strength have been demonstrated due to the moderate cross-linking density of the gel network, few remaining silanol (Si–OH) groups and a repelling behavior among methyl groups, all of which promote reversible compression-reexpansion (spring-back) after the load is removed.[18)–20)] Despite the application of PMSQ materials in different fields, there are only a few reports on PMSQ materials with controllable mesopores. Traditional methods such as supramolecular templating using surfactant, in spite of the prominent success in silica systems,[21)–24)] find difficulties in the formation of mesopores during the direct sol–gel synthesis from methyltrimethoxysilane (MTMS), due to the limited availability of silanol groups that take the crucial role to assemble the system into a mesophasic structure through the strong hydrogen bonding between the polymerizing network and the surfactant.

More importantly, hierarchical porosity with multiple discrete pore sizes, especially in the range of macro- (>50 nm) and mesopores (2–50 nm), is well known to enhance the mass transport and accessible surface area across the material.[25),26)] In particular, it is crucial to enhance the contact between analyte molecules and pore surface by an adequate control of these pores for better separation functions in separation media for high-performance liquid chromatography (HPLC).[25),27)] We[15)] and Dong et al.[28)] reported the preparation of PMSQ materials with well-defined macropores that are characterized by co-continuous structure formed through polymerization-induced phase separation in parallel with sol–gel transition in the absence of surfactant, though the hierarchically macro-mesoporous PMSQ was found to be challenging. Instead, Dong et al. obtained PMSQ monolithic gels only with mesopores without template in the same synthetic framework, which is similar to the "non-templated" silica gels with interstices between colloidal constituents, though the con-

† Corresponding author: K. Kanamori; E-mail: kanamori@kuchem.kyoto-u.ac.jp
†† Corresponding author: K. Nakanishi; E-mail: kazuki@kuchem.kyoto-u.ac.jp
††† Preface for this article: DOI http://dx.doi.org/10.2109/jcersj2.123.P9-1

DOI http://dx.doi.org/10.2109/jcersj2.123.770

trollability of mesopore size was limited and no hierarchically porous PMSQ has been reported in these papers.[28),29)] In contrast to the silica systems,[25),30)] the lack of strong attractive interactions as described above makes the introduction of mesopores in such phase separation systems unrealistic. Alternatively, mesopores may be formed as interstices between gel colloids in the macropore skeletons in the phase separation systems. In the PMSQ systems, however, this strategy is also difficult so far because less aqueous solvent, which mainly leads to mesopores after drying, can be included in the macropore skeletons because of the high hydrophobicity of PMSQ network. As an extension of the above-mentioned PMSQ aerogel systems,[18)–20)] where phase separation is effectively suppressed with the aid of surfactant in the large amount of solvent, we recently succeeded in the synthesis of hierarchically porous PMSQ monoliths with controlled macropores and less-controlled mesopores in the presence of Pluronic F127 ($EO_{106}PO_{70}EO_{106}$, where EO and PO denote ethylene oxide and propylene oxide units, respectively).[31)] The mesopore size in the hierarchically porous PMSQ is, however, limited to 10–20 nm with rather broad distributions, and independent control of macro- and mesopores are not achieved. Hence, the better control over the mesopore parameters such as size and volume while maintaining well-defined co-continuous macroporous structure still remains a challenging task in the PMSQ system.

In this research, aiming at the better controls over mesostructures of PMSQ gels with well-defined co-continuous macropores, incorporation of different Pluronic-type surfactants in the sol–gel process accompanied by phase separation and hydrothermal post-treatment under basic conditions have been investigated. Co-continuous macroporous PMSQ monoliths with controlled mesopore size and volume over a broad range (10 to 60 nm and 0.2 to 0.6 $cm^3 g^{-1}$, respectively) have been successfully obtained. The different strength of interaction between the polymerizing PMSQ network and the surfactants leads to the freezing of gel networks with different connectivity, which changes the mesopore size and volume. In addition, the hydrothermal treatment further leads to the modification in the mesopore characteristics possibly through the partial dissolution-reprecipitation and rearrangement of the siloxane network. The obtained PMSQ monoliths were heat-treated at 250°C to remove the surfactants and processed into monolithic HPLC columns to evaluate the separation performances. High potential for separation in both the reversed-phase and normal-phase modes has been demonstrated with an identical PMSQ monolith. Strong interaction between analyte molecules and retention sites in the gel network has been observed, while hydrophobic interaction between analytes and the methyl groups is stronger than polar-polar interaction between analytes and the silanol groups, due to the further decrease of silanol groups after the hydrothermal treatment as well as the hydrophobic nature of the PMSQ network.

2. Experimental

2.1 Reagents

Methyltrimethoxysilane (MTMS) as the silicon source was purchased from Shin-Etsu Chemical Co. Ltd. (Japan). Triblock copolymers with different ethylene oxide (EO) to propylene oxide (PO) ratios and chain lengths, Pluronic F108 ($EO_{132}PO_{50}EO_{132}$, $M_w = 14600$), F127 ($EO_{106}PO_{70}EO_{106}$, $M_w = 12600$), P105 ($EO_{37}PO_{56}EO_{37}$, $M_w = 6500$) and P123 ($EO_{20}PO_{70}EO_{20}$, $M_w = 5800$) were purchased from Sigma-Aldrich Co. LLC (USA) and used as the surfactant to control phase separation in the sol–gel process. Acetic acid (HOAc, 99.7 wt%) as the catalyst for the hydrolysis of MTMS, urea as the base source during the condensation and tetraethylammonium hydroxide (TEAOH) as the base for hydrothermal treatment were obtained from Kishida Chemical Co., Ltd. (Japan), Hayashi Pure Chemical Ind., Ltd. (Japan) and Tokyo Chemical Industry Co., Ltd. (Japan), respectively. All the chemicals were of analytical grade and used without further purification.

2.2 Synthesis of PMSQ monoliths

In a typical run, 0.7 g of surfactant and 1 g of urea were dissolved in 12 mL of 5 mM HOAc, followed by the addition of 10 mL of MTMS (with [water]/[MTMS] ~ 9.5) under vigorous stirring. A homogeneous solution was obtained after stirring for 30 min for hydrolysis, which was then transferred to a reaction vessel. The vessel was then sealed and left in a 60°C oven for gelation under a static condition. After gelation, the obtained gel was aged at the same temperature for 48 h, and then some of the wet gels were transferred to a Teflon-lined autoclave for further aging under different hydrothermal conditions for 24 h. The obtained gel was washed with methanol for three times (more than 4 h per each time) to remove the surfactant and other unnecessary compounds, followed by drying at 40°C. In some cases, a part of as-dried gel was heat-treated at 250°C to thoroughly remove the surfactant. Monolithic gels for HPLC column were all hydrothermally treated at 120°C for 24 h, washed with methanol, dried at 40°C and heat-treated at 250°C for 2 h.

2.3 Characterizations

Macroscopic and mesoscopic morphologies of the monolithic samples were observed by scanning electron microscopy (SEM, JSM-6060S, JEOL, Japan) and field emission scanning electron microscopy (FE-SEM, JSM-6700F, JEOL, Japan). Meso- and micropore properties of the samples were characterized by nitrogen adsorption–desorption (BELSORP-mini II, Bel Japan Inc., Japan). Samples were heat-treated at 250°C for 2 h and then degassed under reduced pressure at 200°C for more than 4 h before each measurement. Thermal properties of the samples were investigated by thermogravimetry-differential thermal analysis (TG–DTA, Thermal Plus TG 8120, Rigaku Co., Japan) with a continuous air supply at 100 mL min^{-1} and a heating rate at 5°C min^{-1}. The pH values of solutions for hydrothermal treatment were measured by a pH meter (D-50 series, Horiba Inc., Japan). The interaction between surfactant and the PMSQ network was discussed based on the measurements of ^{29}Si cross-polarization magic-angle spinning nuclear magnetic resonance (CPMAS NMR) performed at room temperature in a magnetic field of 7 T using an OPENCORE NMR spectrometer[32),33)] with a 5 mm MAS probe. The carrier frequency and sample spinning frequency for ^{29}Si were 59.506977 MHz and 5 kHz, respectively, and the contact time was 10 ms.

2.4 Chromatographic measurements

Column-shaped PMSQ monoliths, which were prepared in a polypropylene tube with inner diameter of 6 mm, were fabricated into the monolithic HPLC columns by cladding with epoxy resin in a tube with end fittings at both ends. Liquid chromatographic evaluations were carried out using an ordinary HPLC system with a pump (LC-10ADvp, Shimadzu Corp., Japan), an ultraviolet (UV) detector (MU701, GL Sciences Inc., Japan), a data processor (EZ Chrom Elite Chromatography Data System, Agilent Technologies, USA), and an injector (8125, Rheodyne, USA). The system was operated in the isocratic mode at room temperature (~25°C).

3. Results and discussion

3.1 Effect of starting composition on micro/mesopores

The system with surfactant F127 was chosen to show the effects of starting composition on both macropores and mesopores. Detailed starting compositions and SEM images are shown in **Table 1** and **Fig. 1**, respectively. After the acid-catalyzed hydrolysis of MTMS at room temperature, urea is hydrolyzed to generate ammonia at 60°C to promote base-catalyzed polycondensation; this reaction is thus denoted as the acid-base two-step process. Aging of all the gels was carried out at 60°C in the mother liquid for 72 h. Co-continuous macroporous structure can be obtained from optimized starting compositions. Tuning of average macropore size from 1 to 3 μm is possible simply by changing the amount of urea [Figs. 1(A) and 1(B)] or F127 [Figs. 1(D) and 1(B)]. Macropore size decreases when the amount of urea or F127 is increased. An excess amount of either urea or surfactant leads to the formation of a gel without macropores in the micrometer range [Figs. 1(C) and 1(E)]. As compared to surfactant and urea, the change of the amount of HOAc aq. has a reverse effect on the macropore size [Figs. 1(F), 1(B) and 1(G)], i.e. the larger amount increases the macropore size.

The detailed mechanism for the morphology change upon the change in the amount of F127 is explained as the suppression of phase separation in our previous research,[31] and the effect of the amounts of urea and HOAc can be explained in a similar manner as follows. During the polycondensation of hydrolyzed alkoxysilane precursor, phase separation due to the increasing hydrophobicity of MTMS-derived condensates develops in parallel to sol–gel transition. The temporal structure of phase separation consisting of three-dimensionally connected fluid-rich and gel-rich phases is frozen by gelation, resulting in a co-continuous macroporous gel after getting rid of the fluid phase. The hydrolysis of urea at the second step increases pH of the solution, which accelerates the sol–gel transition; the more urea is added, the shorter the gelation time will be. The increase of the amount of urea therefore leads to the formation of gel at the earlier stage of phase separation, resulting in a monolith with smaller macropores. Furthermore, a monolith without macropores in the micrometer range is obtained when excessive amount of urea is added [Fig. 1(C)]. The increase of the amount of HOAc aq. retards the gelation, resulting in an increase in the phase separation tendency and thus larger macropore size [Figs. 1(F), 1(B) and 1(G)]. Since the amounts of surfactant, urea and HOAc aq. have different effects on macropore size, the starting composition for co-continuous macroporous structure can be extended to a broader range [Figs. 1(H) and 1(I)] as compared to the acid one-step process without surfactant reported previously.[15]

Table 1. Starting compositions for PMSQ gels in F127 system[a]

Sample name	Surfactant/g	5 mM HOAc/mL	Urea/g
F127-70-120-5	0.70	12.0	0.50
F127-70-120-10	0.70	12.0	1.00
F127-70-120-15	0.70	12.0	1.50
F127-65-120-10	0.65	12.0	1.00
F127-75-120-10	0.75	12.0	1.00
F127-70-116-10	0.70	11.6	1.00
F127-70-130-10	0.70	13.0	1.00
F127-80-130-10	0.80	13.0	1.00
F127-90-144-10	0.90	14.4	1.00

a) The amount of MTMS was fixed as 10 mL for all the samples.

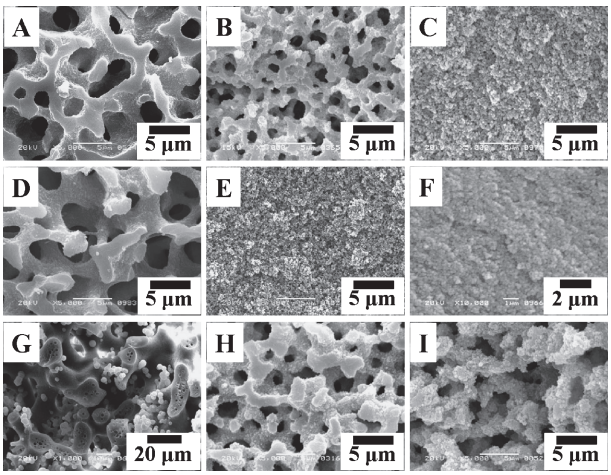

Fig. 1. SEM images of PMSQ gels synthesized with Pluronic F127 as the surfactant at different starting compositions (A: F127-70-120-5, B: F127-70-120-10, C: F127-70-120-15, D: F127-65-120-10, E: F127-75-120-10, F: F127-70-116-10, G: F127-70-130-10, H: F127-80-130-10, and I: F127-90-144-10, from top to bottom in Table 1).

Details concerning the mesostructure of the PMSQ gels were revealed by nitrogen adsorption-desorption measurement and are shown in **Fig. 2** and **Table 2**. The type IV isotherm, which is typical for mesoporous solids, is obtained for all the samples. When the amount of urea (F127-70-120-5, F127-70-120-10) or surfactant (F127-65-120-10, F127-70-120-10) was increased, both mesopore size D_p as well as mesopore volume V_p increased while the hysteresis changed from H2 type (ink bottle type, mesopore with small entrance) to slanted H4 (cylinder type with a broad size distribution) or H3 type (slit type). In terms of micropores, the increase of urea leads to the slight decrease of uptake at relative pressure < 0.1 and thus microporosity, while the amount of surfactant had no obvious effect. During the phase separation process, PMSQ colloids formed by the growth of oligomers tend to concentrate in the gel-rich phase by the uphill diffusion to form macropore skeletons. The space occupied by the solvent in the skeletons is thus the origin of the mesopores. Due to the suppression of phase separation by increasing F127, the sol–gel transition at a less phase-separated system leads to the freezing of a more loosely packed colloids with more solvent incorporated in the gel phase. Both mesopore size and volume therefore increase in the presence of more F127. Meanwhile, micropores are mainly derived from the removal of F127 that is incorporated in the gel network by hydrogen bonding between silanols and EO units,[20),34),35)] and by hydrophobic interaction between the network and PO units.[36),37)] Since the interaction of methylsiloxane polymers with amphiphilic surfactant is not strong,[37),38)] it can be speculated that the incorporated amount of surfactant in the gel network is dominated by the local interaction between PMSQ and surfactant rather than the overall concentration of surfactant in the solution. The change of the amount of surfactant therefore poses virtually no influences on microporosity. Consequently, BET surface area of the gels synthesized with different amount of F127 remains similar due to the fact that micropores contribute to the surface area the most. Urea is added to increase pH of the solution, and the pH increases faster and to higher values when more urea is present in the solution. Hence, the condensation of unreacted silanols form additional siloxane linkage to make the overall network stiffer in the aging step, which makes the micropores derived from the removal of

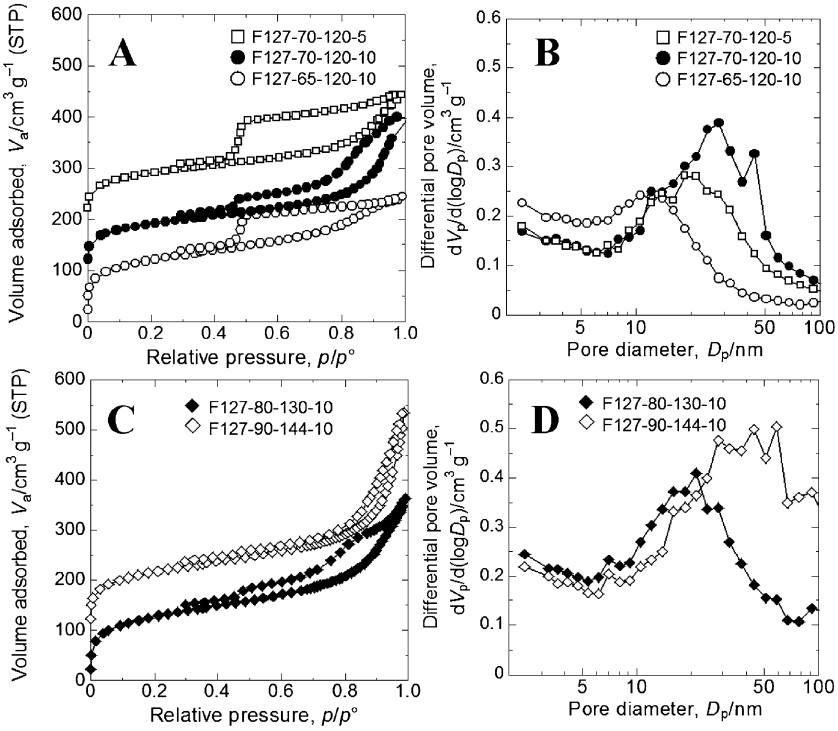

Fig. 2. Nitrogen adsorption–desorption isotherms (each isotherm is shifted vertically by 100 $m^2 g^{-1}$ for clarity) and BJH pore size distributions obtained from the adsorption branch for F127-70-120-5, F127-70-120-10, F127-65-120-10 (A, B) and F127-80-130-10, F127-90-144-10 (C, D).

Table 2. Pore characteristics of PMSQ gels synthesized with F127 as the surfactant

	BET specific surface area a_{BET}/$m^2 g^{-1}$	BJH mesopore volume V_p/$cm^3 g^{-1}$	BJH pore diameter D_p/nm
F127-70-120-5	430	0.27	11
F127-70-120-10	330	0.36	28
F127-65-120-10	320	0.30	18
F127-80-130-10	460	0.45	21
F127-90-144-10	420	0.57	59

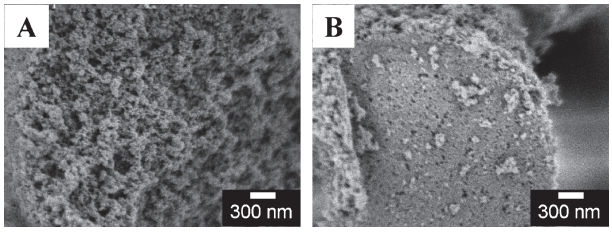

Fig. 3. FE-SEM images of F127-80-130-10 at the (A) surface and (B) cross-section of the macropore skeletons.

surfactant decreased while more mesopores survive after the drying process. The shape change of the mesopores suggested from Fig. 2(C) can be explained by the rearrangement within the macropore skeletons[39] composed of the colloids rather loosely interconnected due to the presence of hydrogen-bonding surfactant. When both the amount of surfactant and water were increased, the mesopore size (21 to 59 nm) and mesopore volume (0.45 to 0.57 $cm^3 g^{-1}$) were further increased due to the synergic effects from the inhibition of phase separation by F127 and the more incorporation of solvent in the gel-rich phase [Figs. 2(C) and 2(D) and Table 2]. The presence of mesopores both on the surface [**Fig. 3**(A)] and inside [Fig. 3(B)] of the macropore skeletons was confirmed by FE-SEM observation.

3.2 Effect of hydrothermal aging on micro/mesopores

Using the gel from the starting composition of F127-70-120-10 after aging at 60°C for 48 h, the mesopore structure was investigated after the additional aging in the mother liquid for 24 h under hydrothermal conditions at different temperatures [120, 150 and 180°C, **Figs. 4**(A) and 4(B)]. Mesopore size increased from 16 to 33 nm together with a slight decrease of microporosity as hydrothermal temperature increased from 120 to 180°C, and the BET surface area therefore decreased from 390 to 320 $m^2 g^{-1}$ [Fig. 4(B) and **Table 3**]. Similar results were observed when F127-80-130-10 was used for aging and the hydrothermal treatment at 60 and 120°C, respectively [Figs. 4(C) and 4(D) and Table 3]. As is confirmed from ^{29}Si CPMAS NMR shown in **Fig. 5**, as the temperature is increased from 60 to 120°C in the hydrothermal treatment on F127-80-130-10, the relative intensity of T^2 [$Si(OSi\equiv)_2(OH)(CH_3)$], which leaves one unreacted silanol group, decreases as compared to the fully condensed T^3 [$Si(OSi\equiv)_3(CH_3)$]. At higher hydrothermal temperature, more activation energy is provided to allow the further condensation of the remaining silanol groups, which leads to the decrease of microporosity. At the same time, partial dissolution of the siloxane network and reprecipitation on the silanol sites may occur, as well known as the Ostwald ripening for the silica system, even if the relative kinetics of dissolution–precipitation may be slower because of the higher hydrophobicity and alkaline resistivity in PMSQ. This ripening effect also contributes to the decrease of micropores with an enlargement of mesopores.

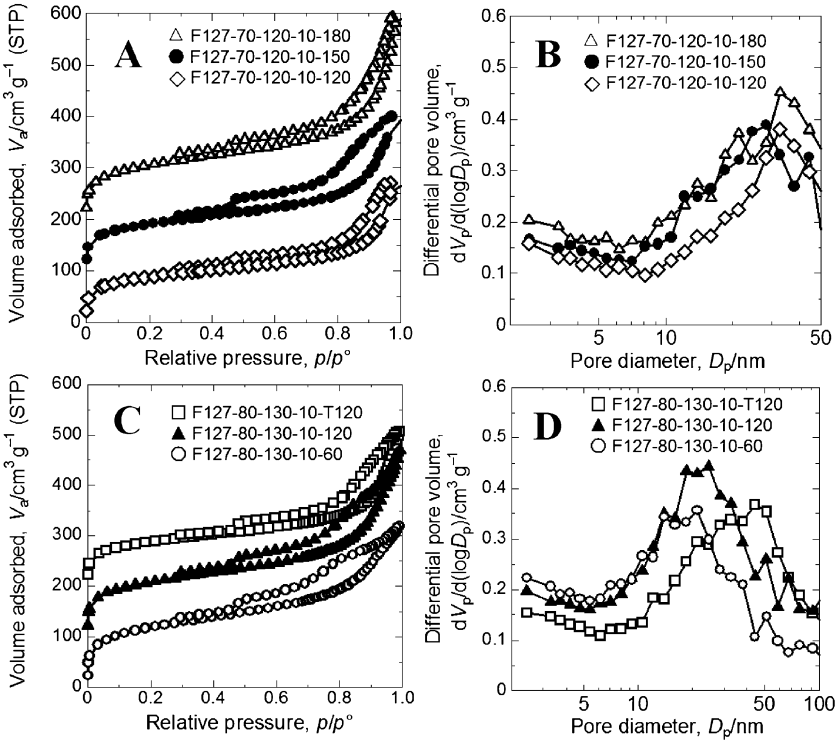

Fig. 4. Nitrogen adsorption–desorption isotherms and BJH pore size distributions obtained from the adsorption branch for the samples hydrothermally treated at different temperatures for 24 h (A, B) and hydrothermally treated in different solutions (C, D). See Table 3 for conditions of hydrothermal treatment.

Table 3. Pore characteristics of PMSQ gels aged at different conditions

	a_{BET}/m^2 g^{-1}	V_p/cm^3 g^{-1}	D_p/nm
F127-70-120-10-120[a)]	390	0.40	16
F127-70-120-10-150	330	0.46	28
F127-70-120-10-180	320	0.60	33
F127-80-130-10-60	430	0.50	21
F127-80-130-10-120	390	0.59	24
F127-80-130-10-T120[b)]	320	0.46	44

a) The last numbers represent the temperature of the hydrothermal treatment. b) Hydrothermal treatment performed in 1 wt% TEAOH at 120°C for 24 h.

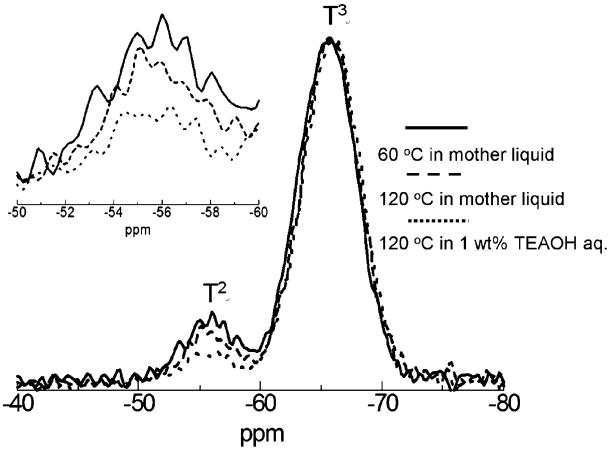

Fig. 5. ^{29}Si CPMAS NMR spectra of the MSQ gel (F127-80-130-10) aged at different conditions.

The comparison among hydrothermal treatment in the solvents with different basicity was studied with F127-80-130-10 at 120°C [Figs. 4(C) and 4(D)]. The increase of pH from 8.2 to 13.3 by changing the hydrothermal solution from mother liquid to 1 wt% tetraethylammonium hydroxide (TEAOH) aqueous solution leads to the increase of mesopore size and decrease of mesopore volume, microporosity and BET surface area (Table 3). The increase of pH imposes a similar effect on microporosity and mesopore size as that of increased urea. As can be seen from Fig. 5, when the gel was treated in 1 wt% TEAOH solution, the relative intensity of T^2 peak further decreases as compared to the case of mother liquid, which indicates the elimination of more silanol groups at higher pH, leading to the further decrease of micropores. The decrease of mesopore volume, moreover, can be attributed to enhanced rearrangement into denser packing of the colloids that form the macropore skeletons, resulting in the decrease of mesopore volume.

3.3 Effect of other surfactants on micro/mesopores

In addition to F127, other amphiphilic surfactants including F108 ($EO_{132}PO_{50}EO_{132}$, $M_w = 14600$), P105 ($EO_{37}PO_{56}EO_{37}$, $M_w = 6500$) and P123 ($EO_{20}PO_{70}EO_{20}$, $M_w = 5800$) were employed to synthesize hierarchically porous PMSQ monoliths. Their interaction with MSQ network and influences on phase separation have been discussed in our previous research;[40] in short, P123 is incorporated in the MSQ network due to its high hydrophobicity, P105 is mainly distributed at the interface of MSQ network and fluid phase, and F108 and F127 tend to be excluded from the network but strong hydrogen bonding with silanols remains as aforementioned. **Figure 6** shows the SEM images of typical macroporous PMSQ gels synthesized with these surfactants and the detailed starting compositions are shown

in **Table 4**. Similar to the case with F127, by simply changing the amount of surfactant or urea to tune the timing between sol–gel transition and phase separation, co-continuous macroporous monoliths were obtained when F108 or P105 were used as the surfactant instead of F127 (Fig. 6). In the case of P123, however, macroscopic precipitation was observed, which later transformed into a monolithic gel with isolated macroporous structure (Fig. 6). Thermal analysis was conducted for all the samples to discuss the distribution of surfactants as a result of the phase separation and gelation (**Fig. 7**). Two-step weight loss in the TG curve together with an exothermic peak in the DTA curve at the second weight loss is observed for all the samples. The first weight loss appearing from 130 to 180°C can mainly be attributed to the decomposition of unreacted urea[41] incorporated in the gel phase, while the second weight loss accompanied by the heat release is due to the combustion of the surfactant embedded in the gel network. The distribution tendency described above is supported by the TG–DTA data; a larger fraction of P123 (67%) is incorporated in the gel phase, while fewer for the others (P105: 61%, F127: 44% and F108: 51%). Micropores and mesopores were evaluated by nitrogen adsorption–desorption on the PMSQ gels synthesized with different surfactants (**Fig. 8**). Relatively high BET surface area (490 $m^2 g^{-1}$) and increased mesopore size and volume (16 nm and 0.61 $cm^3 g^{-1}$) with higher homogeneity are confirmed in the sample prepared with P105.

Among all these surfactants, the ratio of hydrophobic PO units to hydrophilic EO units increases in the order of F108 < F127 < P105 < P123. As the condensation of MSQ oligomers proceeds, the dominant interaction between surfactant and the oligomers changes gradually from the hydrogen bonding between EO units and silanols to hydrophobic interaction between PO units and methyl groups.[40] In the case of F108, the low PO/EO ratio indicates the stronger interaction between the surfactant and the gel network in the earlier stage and weaker interaction in the later stage of polycondensation. As a result, during the phase separation, a higher fraction of the surfactant would be expelled from the gel network into the fluid phase. In other words, less solvent is incorporated in the gel-rich phase, which results in denser gel network with lower BET surface area and decreased mesopore size and volume (**Table 5**). All of the BET surface area, mesopore size and volume increased when PO/EO ratio increases from F108 to F127 and P105 for the same reason. In the case of P123, however, the hydrophobic interaction between P123 and PMSQ network is dominant and hydrogen bonding between P123 and silanols is negligible due to the high PO/EO ratio and short EO chains. The P123 molecules tend to be

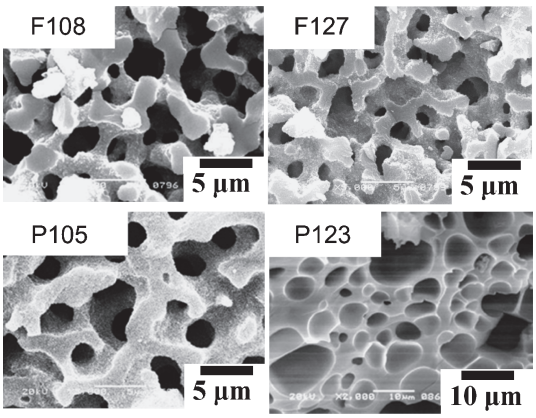

Fig. 6. SEM images of typical macroporous PMSQ gels synthesized with different surfactant; F108-72-120-10, F127-68-120-10, P105-126-120-60 and P123-126-120-60. See Table 4 for starting compositions.

Table 4. Starting compositions for PMSQ gels prepared with different surfactants[a)]

Sample name	Surfactant/g	5 mM HOAc/mL	Urea/g
F108-72-120-10	0.72	12.0	1.00
F127-68-120-10	0.68	12.0	1.00
P105-126-120-60	1.26	12.0	6.00
P123-126-120-60	1.26	12.0	6.00

a) The amount of MTMS was fixed as 10 mL for all the samples.

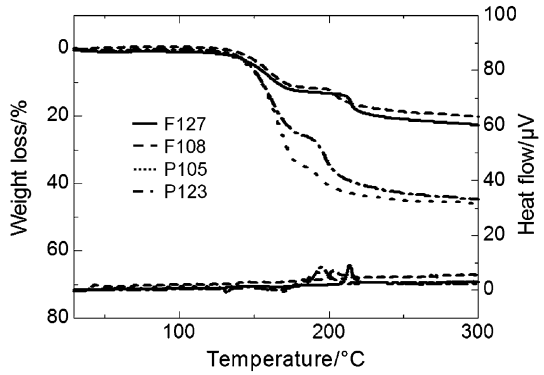

Fig. 7. TG–DTA curves of PMSQ gels synthesized with different surfactants. See Table 4 for starting compositions.

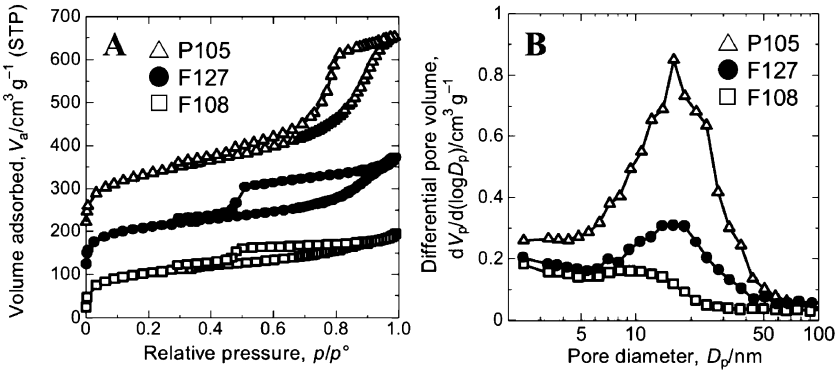

Fig. 8. (A) Nitrogen adsorption desorption isotherms and (B) BJH pore size distributions obtained from the adsorption branch of PMSQ gels synthesized with different surfactants. See Table 4 for starting compositions. All the gels were hydrothermally treated at 120°C in the mother liquid for 24 h before measurement.

Table 5. Pore characteristics of PMSQ gels synthesized with different surfactants[a)]

	$a_{BET}/m^2\,g^{-1}$	$V_p/cm^3\,g^{-1}$	D_p/nm
F108-72-120-10-120	370	0.20	8
F127-68-120-10-120	390	0.32	16
P105-126-120-60-120	490	0.61	16

a) The gels were hydrothermally treated in the mother liquid at 120°C for 24 h before measurement.

Table 6. Calculated values of retention factor for methyl benzoate (k_{1R}), naphthalene (k_{2R}) in the reversed-phase mode and nitrobenzene (k_{1N}) and *o*-nitroanisole (k_{2N}) in the normal-phase[a)]

	Reversed-phase mode		Normal-phase mode	
	k_{1R}	k_{2R}	k_{1N}	k_{2N}
F108-72-120-10-120	0.86	1.68	0.58	1.37
F127-68-120-10-120	0.81	1.79	0.47	1.00
P105-126-120-60-120	1.00	2.22	0.41	0.89

a) Retention factor calculated as $(t - t_0)/t_0$, where t_0 is the retention time of uracil in the reversed-phase mode or that of amylbenzene in the normal-phase mode.

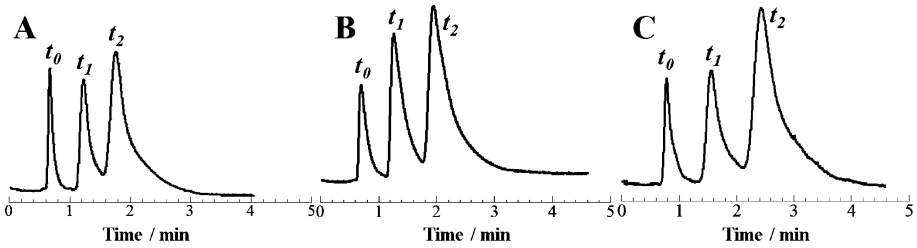

Fig. 9. Chromatograms of the reversed-phase mode HPLC separation of uracil (t_0), methyl benzoate (t_1) and naphthalene (t_2) using PMSQ monolithic columns synthesized with different surfactants; (A) F108-72-120-10-120, (B) F127-68-120-10-120 and (C) P105-126-120-60-120. Conditions: mobile phase acetonitrile/water = 60/40 (v/v), flow rate 1.0 mL min^{-1}, detector UV254 nm, column length 83 mm, temperature 25°C.

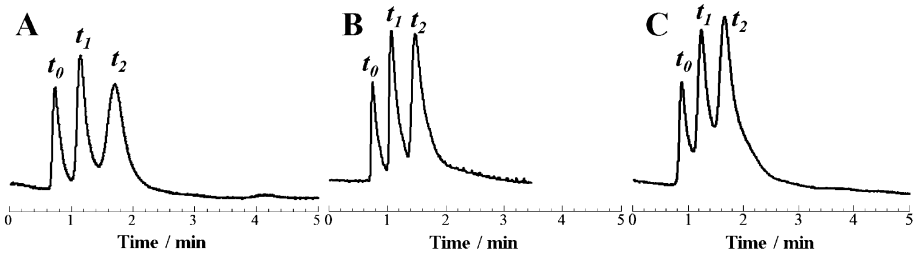

Fig. 10. Chromatograms of the normal-phase mode HPLC separation of amylbenzene (t_0), nitrobenzene (t_1) and *o*-nitroanisole (t_2) using the same PMSQ monolithic columns shown in Fig. 9. Conditions: mobile phase hexane/ethanol = 98/2 (v/v), flow rate 1.0 mL min^{-1}, detector UV254 nm, column length 83 mm, temperature 25°C.

distributed to the PMSQ network and the phase separation cannot be suppressed enough as compared to the other surfactants, which leads to macroscopic precipitation during the sol–gel transition.

3.4 Chromatographic separations

Due to the presence of both hydrophobic methyl groups and hydrophilic silanol groups in PMSQ, a single column is expected to show appreciable HPLC retention in both reversed-phase and normal-phase modes.[42)] However, the PMSQ macroporous gels in our previous research either inherently contains only micropores but no mesopores[42)] or the control over mesopore size was not enough.[31)] Applications of previously obtained PMSQ macroporous gels to HPLC were consequently limited.

In this research, by introducing EOPOEO type amphiphilic surfactants such as F108, F127 or P105 together with the hydrothermal post-treatment, the control of mesopore size and volume over a broad range has been successfully achieved. We therefore performed HPLC separation tests in both reversed-phase and normal-phase modes with columns made from the PMSQ monoliths synthesized with different surfactants (Tables 4 and 5). **Figures 9** and **10** show the chromatograms in the reversed-phase separation of uracil, methyl benzoate and naphthalene and in the normal-phase separation of amylbenzene, nitrobenzene and *o*-nitroanisole, respectively. The retention factors of the analytes increased in the reversed-phase mode when PMSQ monoliths with higher BET surface area and mesopore volume were used (Tables 5 and **6**). Meanwhile, the retention factors of analytes in the normal-phase mode show the inverse tendency and are smaller than those in the reversed-phase mode. These experimental results suggest that the mesopore surface offers hydrophobic sites and shows higher affinity with less polar molecules, because the columns both with high mesopore volume and high surface area show higher retention. By contrast, from the fact that the column prepared with F108 exhibits higher retention in the normal phase mode as compared to those prepared with F127 and P105, the micropores offer rather hydrophilic surfaces, because the column prepared with F108 has less mesopore volume and higher fraction of the surface area is contributed from the micropores.

A comparison of the micropore structure with the reported PMSQ gel synthesized without surfactant via an acid one-step process[15)] (denoted as the reference), which was used as the stationary phase in a capillary column in HPLC, is made to

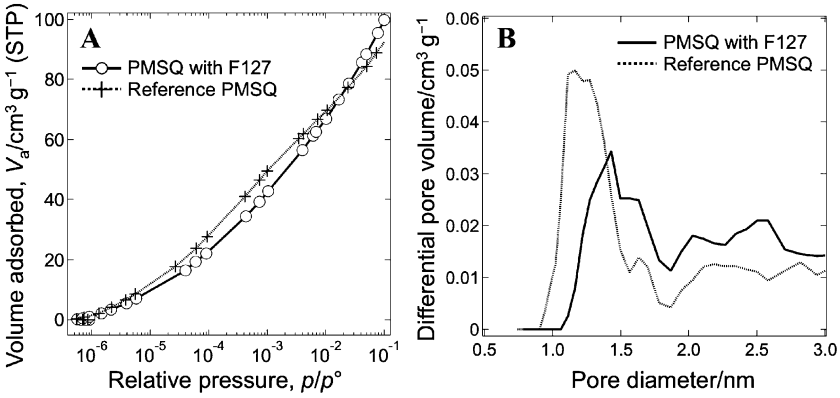

Fig. 11. (A) Logarithmic plot of nitrogen adsorption–desorption isotherms and (B) micropore size distribution calculated by the DFT method of the reference PMSQ material synthesized without surfactant and F127-68-120-10-120 hydrothermally treated at 120°C.

confirm differences in the micropore characteristics in both PMSQ materials. **Figure 11** shows the nitrogen adsorption–desorption isotherms taken in greater detail at the low relative pressure range and micropore size distributions calculated by the density functional theory (DFT) method on F127-68-120-10-120 and the reference. Micropore volume and surface area contributed from the micropore of the reference (0.085 cm^3 g^{-1}, 240 m^2 g^{-1}) are only slightly higher than those in the PMSQ gel synthesized with F127 (0.077 cm^3 g^{-1}, 230 m^2 g^{-1}). The micropore size is, however, smaller with a sharper distribution in the reference [Fig. 11(B)]. From the fact that the reference material suffers from too high retentions in the reversed-phase mode, the micropore surfaces in the present samples are more hydrophilic, presumably because the surfactant molecules that had been anchored by the hydrogen bonding leave more silanol groups on the micropore surface.

In general, the presence of excess amount of micropores leads to the extended trapping of a part of the analyte molecules in the confined space. Such molecules are gradually released by diffusion, which gives rise to the strong tailing in the chromatograms as is found in Figs. 9 and 10. In addition, because of the inhomogeneity of macropore size caused by the rather viscous starting solution, the retention peaks for the analytes are broadened in both separation modes. Hence, by the improvement of the homogeneity of macropore size by decreasing viscosity and elimination of micropores by the hydrothermal treatment in a more basic solution, an improvement of peak width as well as tailing can be expected. In other cases, the strong enough interaction between analytes and retention sites demonstrated here may be beneficial for other analytical applications such as solid phase extraction and refinement of proteins.

4. Conclusions

In this research, synthesis of hierarchically porous PMSQ monoliths with controlled mesopore size and volume over a broad range (10 to 60 nm, 0.2 to 0.6 cm^3 g^{-1}) has been demonstrated for the first time by using EOPOEO-type amphilphilic surfactants (Pluronic F108, F127, P105) and hydrothermal treatment in basic aqueous medium. Interactions between PMSQ network and surfactant contribute to suppression of phase separation and relatively loosely packed gel network, which enlarges the mesopore size and volume. Meanwhile, the effect of hydrothermal treatment includes the partial dissolution-reprecipitation of the siloxane network accompanied by rearrangement of the colloidal network, leading to the extended changes in mesopore size, volume and shape. The obtained PMSQ monoliths have been heat-treated at 250°C to remove the surfactants and processed into HPLC columns to subject to HPLC separation tests in both reversed-phase and normal-phase modes. Strong interaction between analyte molecules and retention sites (methyl groups for reversed-phase mode and silanol groups for normal-phase mode) in the gel network has been demonstrated, indicating the high potential of hierarchically porous PMSQ monolith for analytical purposes. Applications of the PMSQ materials in other fields such as ultralow-k dielectric materials and catalyst supports can also be expected due to the enhanced controllability of pores.

Acknowledgements This work was supported by a Grant-in-Aid for Scientific Research (No. 24550253) administrated by the Japan Society for the Promotion of Science (JSPS) and the Ministry of Education, Culture, Sports, Science and Technology (MEXT) (Japan). Also partially supported by Advanced Low Carbon Technology Research and Development Program (ALCA) administrated by Japan Science and Technology.

References

1) A. P. Wight and M. E. Davis, *Chem. Rev.*, 102, 3589–3614 (2002).
2) F. Hoffmann, M. Cornelius, J. Morell and M. Fröba, *Angew. Chem., Int. Ed.*, 45, 3216–3251 (2006).
3) C. Sanchez, P. Belleville, M. Popall and L. Nicole, *Chem. Soc. Rev.*, 40, 696–753 (2011).
4) T. Shimada, K. Aoki, Y. Shinoda, T. Nakamura, N. Tokunaga, S. Inagaki and T. Hayashi, *J. Am. Chem. Soc.*, 125, 4688–4689 (2003).
5) P. K. Jal, S. Patel and B. K. Mishra, *Talanta*, 62, 1005–1028 (2004).
6) S. S. Park and C. Ha, *Chem. Rec.*, 6, 32–42 (2006).
7) Y. Yeon, Y. J. Park, J. Lee, J. Park, S. Kang and C. Jun, *Angew. Chem., Int. Ed.*, 47, 109–112 (2008).
8) J. Park and C. Jun, *J. Am. Chem. Soc.*, 132, 7268–7269 (2010).
9) N. Moitra, S. Ichii, T. Kamei, K. Kanamori, Y. Zhu, K. Takeda, K. Nakanishi and T. Shimada, *J. Am. Chem. Soc.*, 136, 11570–11573 (2014).
10) R. J. P. Corriu and D. Leclercq, *Angew. Chem., Int. Ed. Engl.*, 35, 1420–1436 (1996).
11) K. J. Shea and D. A. Loy, *Chem. Mater.*, 13, 3306–3319 (2001).
12) N. Mizoshita, T. Tani and S. Inagaki, *Chem. Soc. Rev.*, 40, 789–800 (2011).
13) K. Kanamori and K. Nakanishi, *Chem. Soc. Rev.*, 40, 754–770 (2011).

14) J. Zimmermann, F. A. Reifler, G. Fortunato, L. Gerhardt and S. Seeger, *Adv. Funct. Mater.*, **18**, 3662–3669 (2008).
15) K. Kanamori, H. Yonezawa, K. Nakanishi, K. Hirao and H. Jinnai, *J. Sep. Sci.*, **27**, 874–886 (2004).
16) B. Lee, Y. Park, Y. Hwang, W. Oh, J. Yoon and M. Ree, *Nat. Mater.*, **4**, 147–151 (2005).
17) K. Kamiya, "Handbook of Sol-gel Science and Technology: Processing Characterization and Applications", Volume I, Ed. by S. Sakka, Kluwer Academic Publishers, Dordrecht (2004) pp. 185–201.
18) K. Kanamori, M. Aizawa, K. Nakanishi and T. Hanada, *Adv. Mater.*, **19**, 1589–1593 (2007).
19) K. Kanamori, M. Aizawa, K. Nakanishi and T. Hanada, *J. Sol-Gel Sci. Technol.*, **48**, 172–181 (2008).
20) K. Kanamori, K. Nakanishi and T. Hanada, *J. Ceram. Soc. Japan*, **117**, 1333–1338 (2009).
21) T. Yanagisawa, T. Shimizu, K. Kuroda and C. Kato, *Bull. Chem. Soc. Jpn.*, **63**, 988–992 (1990).
22) C. T. Kresge, M. E. Leonowicz, W. J. Roth, J. C. Vartuli and J. S. Beck, *Nature*, **359**, 710–712 (1992).
23) D. Zhao, J. Feng, Q. Huo, N. Melosh, G. H. Fredrickson, B. F. Chmelka and G. D. Stucky, *Science*, **279**, 548–552 (1998).
24) G. J. A. A. Soler-Illia, C. Sanchez, B. Lebeau and J. Patarin, *Chem. Rev.*, **102**, 4093–4138 (2002).
25) K. Nakanishi and N. Tanaka, *Acc. Chem. Res.*, **40**, 863–873 (2007).
26) "Hierarchically Structured Porous Materials", Ed. by B. Su, C. Sanchez and X. Yang, Wiley-VCH, Weinheim (2012).
27) G. Guiochon, *J. Chromatogr. A*, **1168**, 101–168 (2007).
28) H. Dong, M. A. Brook and J. D. Brennan, *Chem. Mater.*, **17**, 2807–2816 (2005).
29) H. Dong and J. D. Brennan, *Chem. Mater.*, **18**, 541–546 (2006).
30) K. Nakanishi, R. Takahashi, T. Nagakane, K. Kitayama, N. Koheiya, H. Shikata and N. Soga, *J. Sol-Gel Sci. Technol.*, **17**, 191–210 (2000).
31) K. Kanamori, Y. Kodera, G. Hayase, K. Nakanishi and T. Hanada, *J. Colloid Interface Sci.*, **357**, 336–344 (2011).
32) K. Takeda, *Rev. Sci. Instrum.*, **78**, 033103 (2007).
33) K. Takeda, *J. Magn. Reson.*, **192**, 218–229 (2008).
34) R. Ryoo, C. H. Ko, M. Kruk, V. Antochshuk and M. Jaroniec, *J. Phys. Chem. B*, **104**, 11465–11471 (2000).
35) M. Kruk, M. Jaroniec, C. H. Ko and R. Ryoo, *Chem. Mater.*, **12**, 1961–1968 (2000).
36) R. J. Green, S. Tasker, J. Davies, M. C. Davies, C. J. Roberts and S. J. B. Tendler, *Langmuir*, **13**, 6510–6515 (1997).
37) S. Yang, P. A. Mirau, C. Pai, O. Nalamasu, E. Reichmanis, E. K. Lin, H. Lee, D. W. Gidley and J. Sun, *Chem. Mater.*, **13**, 2762–2764 (2001).
38) N. Hüsing, D. Brandhuber and P. Kaiser, *J. Sol-Gel Sci. Technol.*, **40**, 131–139 (2006).
39) A. Mushiake, K. Kanamori and K. Nakanishi, *Int. J. Polym. Sci.*, **2012**, 460835 (2012).
40) M. Kurahashi, K. Kanamori, K. Takeda, H. Kaji and K. Nakanishi, *RSC Adv.*, **2**, 7166–7173 (2012).
41) P. M. Schaber, J. Colson, S. Higgins, D. Thielen, B. Anspach and J. Brauer, *Thermochim. Acta*, **424**, 131–142 (2004).
42) K. Kanamori, K. Nakanishi and T. Hanada, *J. Sep. Sci.*, **29**, 2463–2470 (2006).